Journal of Equine Veterinary Science 128 (2023) 104826

Contents lists available at ScienceDirect

Journal of Equine Veterinary Science

journal homepage: www.j-evs.com

Short communication

An *Ex Vivo* Pilot Study to Assess the Feasibility of 3D Printing of Orbital Implants in Horses

Jenny Jarry[a], Yves De Raeve[a], Alexandra Dugdale[b], Vincent Simon[a], Jean-Michel Vandeweerd[a,*]

[a] *Integrated Veterinary Research Unit (IVRU) – Namur Research Institute for Life Sciences (NARILIS), Department of Veterinary Medicine, Faculty of Sciences, University of Namur, Namur, Belgium*
[b] *Paragon Veterinary Referrals, Paragon Business Village, Wakefield, UK*

ARTICLE INFO

Article history:
Received 20 March 2023
Received in revised form 21 May 2023
Accepted 22 May 2023
Available online 26 May 2023

Keywords:
Orbital implant
3D printing
Modified transconjunctival enucleation
Horse
Ophthalmology

ABSTRACT

Severe ophthalmic conditions such as trauma, uveitis, corneal damage, or neoplasia can lead to eye removal surgery. Poor cosmetic appearance resulting from the sunken orbit ensues. The aim of this study was to demonstrate the feasibility of manufacturing a custom-made 3D-printed orbital implant made of biocompatible material for the enucleated horse and usable in conjunction to a corneoscleral shell. Blender, a 3D-image software, was used for prototype design. Twelve cadaver heads of adult Warmbloods were collected from the slaughterhouse. On each head, one eye was removed via a modified transconjunctival enucleation while the contralateral eye was kept intact as control. Ocular measurements were collected on each enucleated eye with the help of a caliper and used for prototype sizing. Twelve custom-made biocompatible porous prototypes were 3D-printed in BioMed Clear resin using the stereolithography technique. Each implant was fixated into the corresponding orbit, within the Tenon capsule and conjunctiva. Heads were frozen and thin slices were then cut in the transverse plane. A scoring system based on four criteria (space for ocular prosthesis, soft-tissue-coverage, symmetry to the septum, and horizontal symmetry), ranging from A (proper fixation) to C (poor fixation), was developed to evaluate implantation. The prototypes reached our expectations: 75% of the heads received an A score, and 25% a B score. Each implant cost approximately 7.30€ and took 5 hours for 3D-printing. The production of an economically accessible orbital implant made of biocompatible porous material was successful. Further studies will help determine if the present prototype is usable *in vivo*.

1. Introduction

Conditions of the eye and its adnexa are common in horses, such as trauma, uveitis, corneal ulcers, nontraumatic keratitis, and ocular and peri-ocular neoplasia [4]. They sometimes lead to irreversible eye damage, blindness, and chronic pain [6]. The patient's quality of life becomes deeply impaired and surgical enucleation, evisceration or exenteration must be performed. Whatever the procedure, the orbit appears sunken afterwards [9]. The poor cosmetic appearance can have negative psychological impacts on people, especially owners [6,14].

Cosmetic solutions have been described [6,9]. Tinted contact lenses can be used when the cornea has been damaged but still retains a normal spherical shape. The eye must be pain-free. Corneoscleral shells can also provide a satisfactory cosmetic appearance. However, the adjustment to the patient's orbit is challenging and the prosthesis must be cleaned regularly. Furthermore, inadvertent loss of the prosthesis is common, and the owner should have a replacement at the ready to avoid eyelid contraction and atrophy [9]. Silicone or polymethyl methacrylate intraocular implants [13,14] can prevent the sunken appearance of the orbit [2]. These types of implants are most commonly used in case of glaucoma or recurrent uveitis, but they are contraindicated in inflammatory conditions such as keratitis and scleritis [6].

In man [7], cosmetic corneoscleral shells fitting in-between the bulbar conjunctival stump and the eyelids are currently used in conjunction to integrated porous orbital implants [1]. Integration and porosity allow for attachment of extra-ocular muscles

Animal welfare/ethical statement: This study is performed on cadavers. It obtained approval from the CEEXPANI (Comité Ethique en Expérimentation Animale) of the University of Namur (Belgium).

* Corresponding author at: Jean-Michel Vandeweerd, Integrated Veterinary Research Unit (IVRU) – Namur Research Institute for Life Sciences (NARILIS), Department of Veterinary Medicine, Faculty of Sciences, University of Namur, Namur, Belgium.

E-mail address: jean-michel.vandeweerd@unamur.be (J.-M. Vandeweerd).

https://doi.org/10.1016/j.jevs.2023.104826
0737-0806/

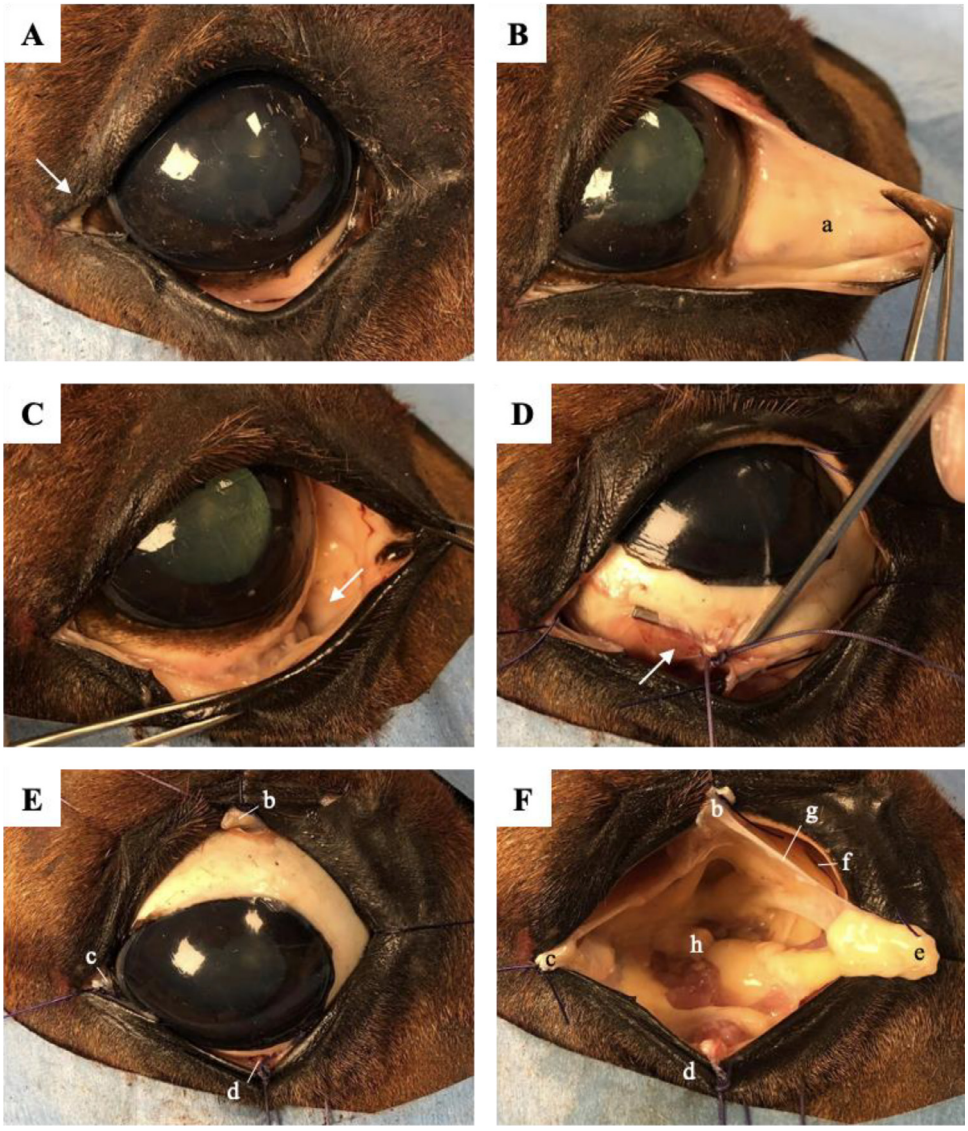

Addendum 1. Modified transconjunctival enucleation. (A) Incision of the lateral canthus to facilitate access to the eyeball, (B) Identification of the nictating membrane, (C) Removal of the nictating membrane, (D) Following a 360° peritomy of the conjunctiva at the limbus, isolation of the four recti muscles (dorsal, medial, ventral, lateral). As shown by the arrow for the ventral recti muscle, each recti muscle was isolated, sutured (PDS 0) and transected between the suture and the eyeball. Oblique muscles were also isolated and left to retract posteriorly. (E) Preservation of each suture connected to the recti muscles before extraction of the eyeball and transection of the optic nerve and retractor bulbi muscle. The fat within the orbit was preserved as much as possible. (F) Removal of the eyeball, (a) Nictating membrane, (b) Dorsal recti muscle, (c) Lateral recti muscle, (d) Ventral recti muscle, (e) Medial recti muscle, (f) Conjunctiva, (g) Tenon capsule, (h) Transected optic nerve.

and fibrovascular growth, aiming to reduce infection risks and to increase fixation of the implant within the orbit. However, combining an orbital implant and a cosmetic ocular prosthesis is expensive and can be prone to complications according to the literature in human medicine. Therefore, such combinations are rarely used in veterinary medicine but deserve further investigation.

In recent years, advances in 3D-printing have made this technology a promising solution for medical planning and prosthesis manufacturing. Low fabrication costs and fast production make it an interesting alternative. A publication in canine medicine has reported the use of 3D-printing to manufacture implants and prostheses [9]. The present *ex vivo* pilot study aimed to describe and assess a 3D-printing technique to produce a low-cost orbital implant made of biocompatible porous material and usable in conjunction to a cosmetic corneoscleral shell.

The heads of twelve (n = 12) adult Warmbloods without eye pathology were collected in a slaughterhouse. One eye (left or right) was enucleated. An incision was made at the lateral canthus of the eye. The nictating membrane was transected. A 360° peritomy was performed to open the conjunctiva and Tenon capsule at the limbus. The anterior part of the capsule was dissociated from the sclera. The four recti muscles were hooked and sutured 5 millimeters distally from their insertion on the eyeball. These muscles were transected between their insertion and the suture. The two oblique muscles were hooked, transected, and left to retract posteriorly. The optic nerve and retractor bulbi muscle were transected. The procedure is illustrated in Addendum 1.

Each enucleated eye was placed in water in a two-liter rectangular container and frozen. Then the ice-cube was sliced with a bandsaw passing through the sagittal plane of the eye. The axial (antero-posterior distance of the globe from the anterior external surface of the cornea to the posterior external surface of the sclera) and vertical (dorso-ventral distance of the globe from the dorsal external surface of the sclera to the ventral external surface of the sclera) globe lengths were measured using a caliper [12] (Addendum 2).

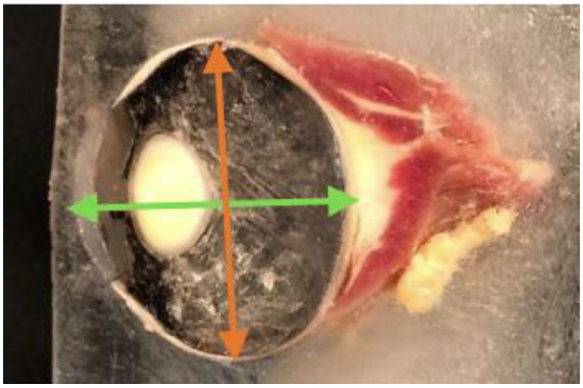

Addendum 2. Axial and vertical globe lengths measurements. Green: Axial (antero-posterior distance of the globe from the anterior external surface of the cornea to the posterior external surface of the sclera) globe length, Orange: Vertical (dorso-ventral distance of the globe from the dorsal external surface of the sclera to the ventral external surface of the sclera) globe length. These measurements were achieved using a caliper.

For the design of the implant, structural features, such as steep mounds, abrasive surfaces or pegs, were avoided since they can cause thinning of the conjunctiva, leading to implant extrusion, infection, discharge or excessive granulomatous tissue formation [3]. Implants for humans and dogs are usually spherical. The implant was shaped as an ellipse to replicate the oblate spheroid shape of the equine globe. It was made porous to allow for fibrovascular growth. The addition of an anterior suture-fixation platform that would offer several suture options for the recti muscles was decided. The four suture tunnels should have a diameter of 2.5 mm to allow easy passage of the suture needle. The final design of the integrated implant prototype for this study was mainly inspired by the canine orbital implant prototype design described by Park et al. [10].

The prototype was designed using a free 3D-image software. Different systems were tested and Blender (Blender Foundation, Amsterdam, Netherlands) was eventually chosen (Fig. 1). The measures anterior globe length (AGL) and vertical globe length (VGL) were used for prototype sizing. Mean AGL and VGL were respectively 42.2 mm (SD 3.9 mm) and 48.8 mm (SD 3.9 mm). Following published data on the ideal size of orbital implants, each implant's volume was scaled to be 20 % smaller than the original eye [8].

Once the prototype design satisfied the chosen standards, it was saved and exported in stereolithography (SLA) format. A Form2 3D-printer (FormLabs) and BioMed Clear resin were used. The latter is a biocompatible rigid material that is reported to sustain long-term skin and mucosal membrane contact without complications. It is also a USP Class VI certified material, FDA approved and compatible with common sterilization methods [15]. After the completion of the printing phase, the prototypes were rinsed using isopropyl alcohol (99%) and then air-dried for 30 minutes at room temperature. Finally, the prototypes were placed for 60 minutes in a post-curing Formlabs unit where temperature was raised at 60°C. These steps insured that the resin reached its described properties. The mean manufacturing price of the implant was 7.30 € and the printing process lasted approximately 5 hours. The implants were then fixed in their corresponding orbit, as described in Fig. 2.

To assess the accuracy of the fixation of the implants, the twelve heads were frozen after implantation, and thin (5–8 mm) slices were performed in the transverse plane using an electric band saw. Four criteria were used to assess the position of the implant: space for a cosmetic ocular prosthesis, soft tissue coverage, horizontal symmetry, and symmetry to the septum (Fig. 3). In man, thin shells (1.5 mm and less) are placed when the eye and its surrounding soft tissue are preserved, whilst full thickness ocular prosthesis (1.5 mm and more) can be used with orbital implants.

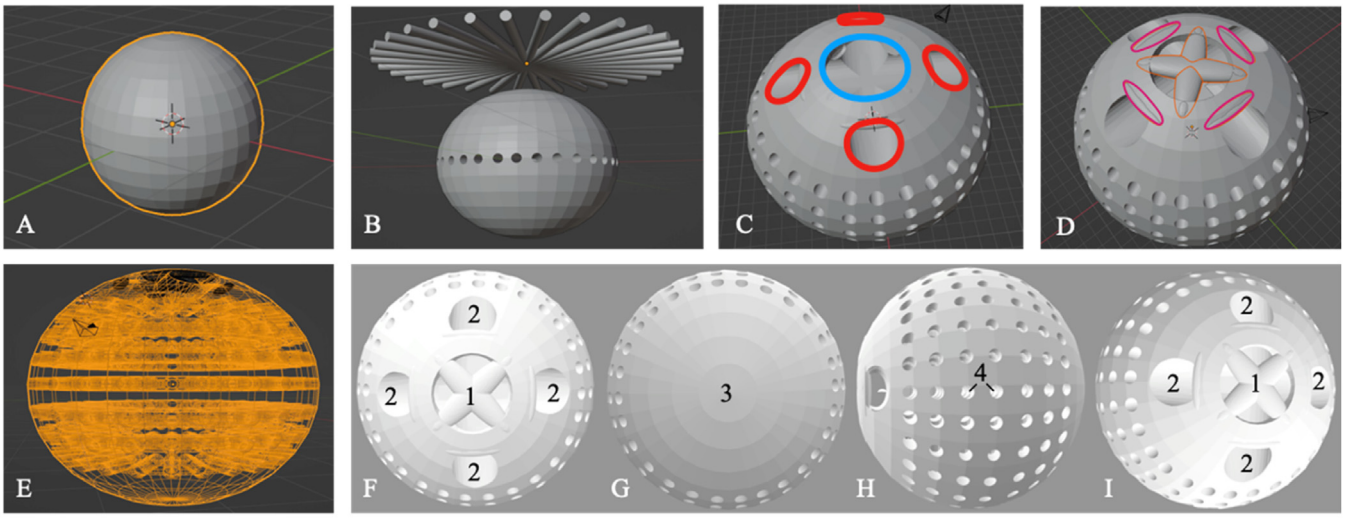

Fig. 1. Design of the prosthesis. (A) Addition and scaling according to equine ophthalmic measurements of a UV sphere mesh on the Blender desktop (U and V represent the bidimensional (2D) projection axes of the 3D design), (B) Addition and superimposition within the ellipse of thirty-two cylinders joined in a star-shaped pattern. The picture shows the sphere after the cylinders were submitted to the boolean modifier. The star-shape pattern is placed above the sphere to show the created porosity. This manoeuver was replicated six times. A small additional UV sphere was placed at the very center of the now porous structure. This ensured the center of the initial sphere was filled with resin. Without the addition of the smaller sphere, the center of the implant would be hollow and could be the source of complications such as fluid collection and bacterial proliferation, (C) Creation of the anterior suture-fixation platform. Two cylinders were added to the desktop, flattened, scaled to fit within the anterior solid part of the ellipse and placed in a cross-like pattern. They were then joined together, superimposed within the ellipse, and submitted to the boolean modifier. The picture shows the created tunnels (red circles) for the suture material once the cylinders were deleted. A small UV sphere mesh was also added to the desktop and superimposed at the very top of the anterior part of the ellipse. This small UV sphere was then submitted to the boolean modifier and deleted to create the anterior circular cavity of the platform (blue circle), (D) Addition of two perpendicularly joined cylinders at the top of the platform to multiply suture options (orange outlines) and of four cylinders at each tunnel's roof opening to avoid sharp edges (pink outlines), (E) Addition of fourteen torus-shaped meshes within the ellipse to join pores around the prototype, F–I = Final production of the stereolithography format file for 3D printing (F) Anterior view, (G) Posterior view, (H) Lateral view, (I) Oblique view, (1) Anterior suture fixation platform, (2) Tunnels for recti muscle fixation, (3) Nonporous posterior face to limit soft tissue irritation, 4: Pores dedicated to fibrovascular growth).

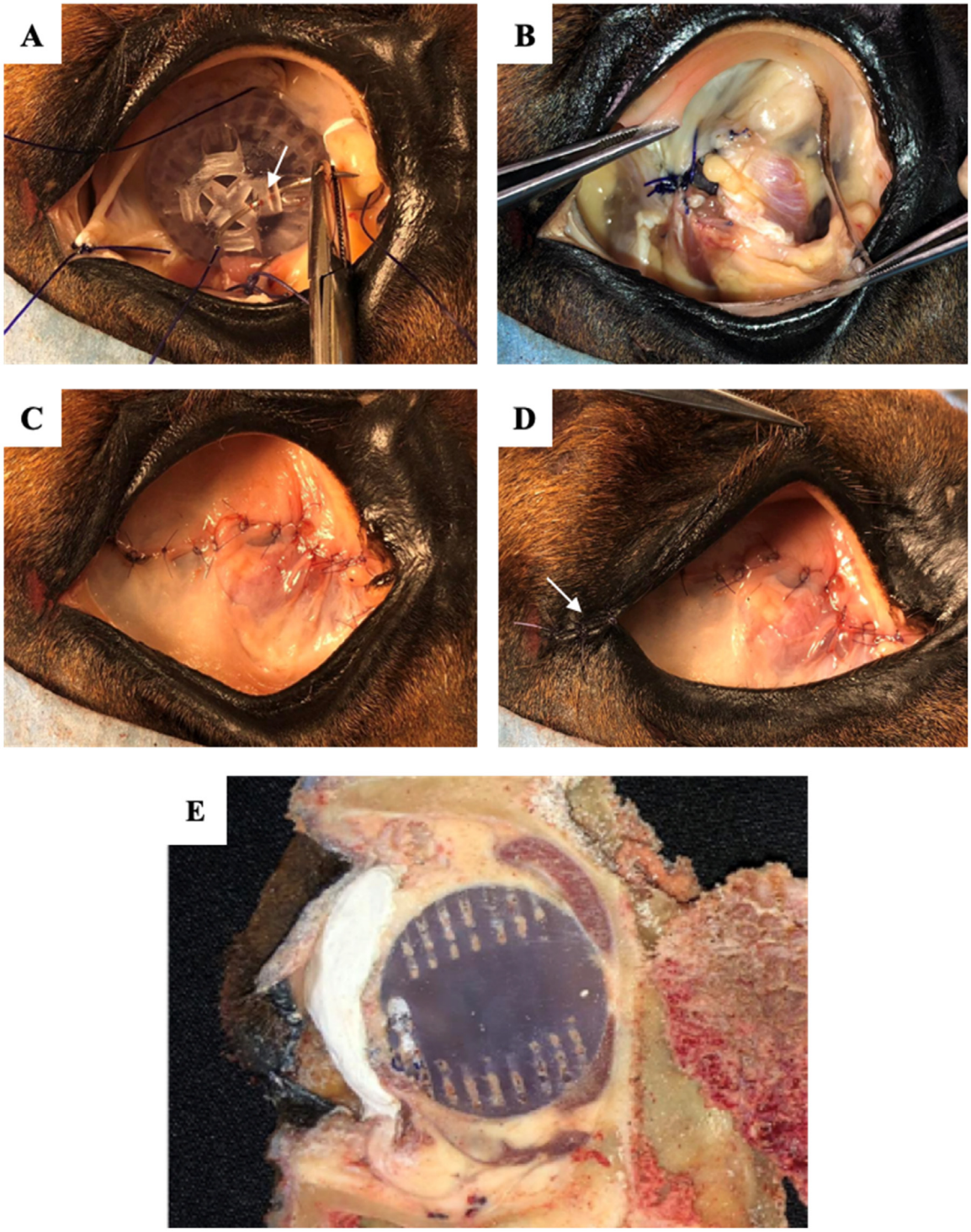

Fig. 2. Implant fixation. (A) Placement of the implant within the Tenon capsule and suturing of the four recti muscles on the platform. The arrow shows the needle passing through one of the implant's suturing tunnels, (B) Suture of recti muscles on the platform (PDS 0) before suturing of the conjunctiva, (C) Suture of conjunctiva (monocryl 5.0), (D) Suture of lateral canthus of the eye (monocryl 3.0), (E) Thin slice in the transverse plane obtained after freezing the head. Plaster has been placed in-between the bulbar conjunctival stump and the eyelids to show the space for the cosmetic ocular prosthesis.

Optimal thickness of the prosthesis will depend on the molding of the space between the eyelids and the bulbar conjunctival stump [11]. According to the moldings performed during this study, thickness of cosmetic ocular prosthesis used with the prototype should range from 4 to 8 mm.

Nine heads out of twelve received the highest possible score A and the remaining three heads received an intermediate B score. In addition the needles went through the tunnels without any trouble. This demonstrates that the adaptation and fixation of the prototype within the orbit of the 12 cadaver heads was successful with good soft tissue coverage over the anterior part of the implant and proper fixation within the orbit.

In clinical cases, it could be interesting to use ultrasonography or computed tomography of the contralateral eye for measure-

proper fixation ← → *poor fixation*

EVALUATED CRITERIA		ATTRIBUTED POINTS		
①	**Space for a cosmetic ocular prosthesis**	3 to 8 mm → *2 points*	1.5 to 3 mm or 8 to 10 mm → *1 point*	< 1.5 mm or > 10 mm → *0 point*
②	**Soft tissue (bulbar conjunctiva and muscles) coverage**	≥ 4 mm → *2 points*	2 to 4 mm → *1 point*	< 2 mm → *0 point*
③	**Symmetry to the septum |a-b|**	≤ 6 mm → *2 points*	6 to 12 mm → *1 point*	> 12 mm → *0 point*
④	**Horizontal symmetry**	≤ 2 mm → *2 points*	2 to 4 mm → *1 point*	> 4 mm → *0 point*
FINAL SCORE AFTER POINTS ADDITION		**Score A** *6 to 8 points*	**Score B** *3 to 5 points*	**Score C** *0 to 2 points*

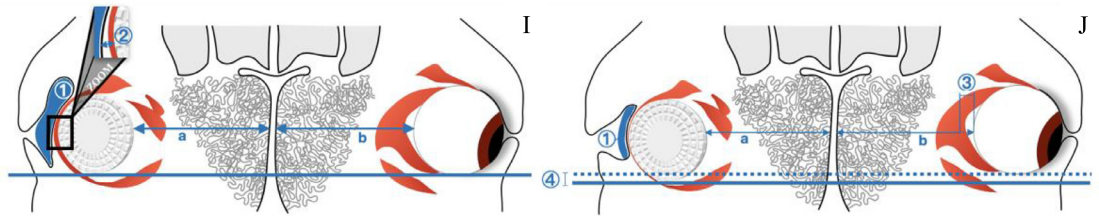

Fig. 3. Assessment scores for orbital implant placement. Each criterion is attributed 0, 1 or 2 points depending on the measurements. The addition of the points obtained for the four criteria provides a score. For example, score A is attributed if the obtained number of points ranges from 6 to 8. I: Properly placed implant, J: Poorly placed implant, (1) Sufficient space left between the sutured bulbar conjunctiva and the eyelids to allow for placement of a cosmetic ocular prosthesis. (2) Soft tissue coverage of the prototype should be sufficient to avoid dehiscence (thickness of conjunctiva plus muscle ≥ 2 mm), (3) Symmetry between implant and contralateral eye assessed by comparing their distances to the nasal septum, (4) Horizontal placement symmetry assessed by comparing positions of implant and intact eye in comparison to a horizontal line perpendicular to the nasal septum drawn at the ventral limit of the ocular globe.

ments. But since the manufacturing costs are low and the resizing process of the stereolithography file is easy, the best option might be to print in advance several implants of various diameters. This would ensure to place the most appropriately sized implant during surgery. Having variously sized implants custom printed and ready for use would allow for unexpected needs in circumstances in which the surgeon is unsure of the size of the eyeball prior to enucleation (i.e., hypotonic eyes) or an extensive portion of soft tissue had to be removed during surgery.

It can be speculated that such implants could be used both in elective enucleation procedures and in enucleations performed as an emergency. The decision to place an orbital implant, however, will depend on the presence of signs of infection. No implantation should be performed for an infected eye, to prevent complications and rejection of the implant [6].

To complete the orbital implant, a cosmetic ocular prosthesis should be fitted in-between the bulbar conjunctival stump and the eyelids. Descriptions of the process in human, equine and canine medicine have been published in the literature [5,10] but were not assessed in the current study.

It is important to note that the prototype described in this study would most likely not be adequate for horses that are presented long after having sustained an enucleation. Soft tissue remodeling would prevent proper fixation of the implant. Not only would the eyelids probably lack muscle tone, but recti muscles would also have retracted posteriorly within the orbital cavity.

BioMed Clear resin was used in this study. It is a photopolymer resin composed of methacrylic esters and photoinitiators. Though it is described as an FDA approved, USP Class VI certified biomaterial, the fabricant specifies that users should independently verify the suitability of the printed materials for their intended purposes. Therefore, monomer leaching of the crosslinkable photopolymer and cytotoxicity should be further investigated. To our knowledge, no data has been published on the eventual effects of these molecules in horses.

The major weakness of the current study is the fact that it was performed *ex vivo*. However, using heads collected in the slaughterhouse is much more ethical than euthanizing experimental horses. In addition, to be able to cut slices in heads, freezing was necessary.

In conclusion, the successful production of an economically accessible and porous orbital implant made of biocompatible material gives perspective to orbital implants in horses and provides new ideas for veterinary ophthalmic surgery. Further studies should help determine whether the present prototype can be used *in vivo*.

Declaration of Competing Interest

The authors declare they have no conflict of interest.

References

[1] Baino F, Perero S, Ferraris S, Miola M, Balagna C, Verné E, Vitale-Brovarone C, Coggiola A, Dolcino D, Ferraris M. Biomaterials for orbital implants and ocular prostheses: Overview and future prospects. Acta Biomaterialia 2014;10:1064–87.

[2] Betbeze CM, Dray SM, Fontenot RL. Subconjunctival enucleation with orbital implant placement in standing horses: 20 cases (2014-2017). J Am Vet Med Association 2021;258:661–7.

[3] Brooks DE. Complications of ophthalmic surgery in the horse. Vet Clin N Am: Equine Pract 2008;24:697–734.

[4] Gilger BC. Equine ophthalmology, Third Edition, 3. Hoboken, New Jersey: Wiley Blackwell; 2017. p. 90–1.

[5] Gilger BC, Pizzirani S, Johnston LC, Urdiales NR. Use of a hydroxyapatite orbital implant in a cosmetic corneoscleral prosthesis after enucleation in a horse. J Am Vet Med Assoc 2003;222:343–5.

[6] Hamor RE, Roberts SM, Severin GA, Trawnik WR, Johnson WJ. Ocular cosmetic and prosthetic devices. Vet Clin N Am: Equine Pract 1992;8:637–54.

[7] Jordan DR, Klapper SR. Controversies in enucleation technique and implant selection: whether to wrap, attach muscles, and peg? Oculoplast orbit 2010:195–211.

[8] Kaltreider SA, Jacobs JL, Hughes MO. Predicting the ideal implant size before enucleation. Ophthal Plast Reconst Surg 1999;15:37–43.

[9] Lavach JD, Severin GA. Equine ocular cosmesis. Vet Clin N Am: Large Animal Pract 1984;6:489–500.

[10] Park SY, An JH, Kwon H, Choi SY, Lim KY, Kwak HH, Hussein KH, Woo HM, Park KM. Custom-made artificial eyes using 3D printing for dogs: a preliminary study. PLoS ONE 2020;15(11):e0242274.

[11] Raizada K, Rani D. Ocular prosthesis. Contact Lens Anterior Eye 2007;30:152–62.

[12] Rogers M, Cartee RE, Miller W, Ibrahim A. Evaluation of the extirpated equine eye using B-mode ultrasonography. Vet Radiol 1986;27(1):24–6.

[13] Romkes G, Eule JC. Followup of a dog with an intraocular silicone prosthesis combined with an extraocular glass prosthesis. Case Rep Vet Med 2012;2012:1–6.

[14] Toth J, Huthmann S, Dikker L. Intrascleral ocular prosthesis following evisceration in thirteen horses. Pferdeheilkunde 2014;2:153–60.

[15] Formlabs [online]. Safety data sheet – According to OSHA Hazard Communication Standard. 2020 [initial preparation date: 05.28.2020; revision date: 02.04.2022]. Available: https://formlabs-media.formlabs.com/datasheets/2001424-SDS-ENUS-0.pdf. [Accessed 15 May 2023].